Int. J. Solids Structures Vol. 19, No. 2, pp. 93–104, 1983
Printed in Great Britain.

0020-7683/83/020093-12$03.00/0

A SOLUTION TECHNIQUE FOR INDIRECT BOUNDARY INTEGRAL EQUATION IN PLANAR ELASTO-PLASTIC PROBLEMS

MADHUKAR VABLE
Mechanical Engineering and Engineering Mechanics, Michigan Technological University, Houghton, MI 49931, U.S.A.

and

DAVID L. SIKARSKIE
Metallurgy, Mechanics and Material Science Department, Michigan State University, East Lansing, MI 48824, U.S.A.

(*Received* 30 *October* 1981; *in revised form* 13 *May* 1982)

Abstract—A scheme for solving planar elasto-plastic problems using the indirect boundary element approach is presented. The area integrals over the plastic region contains singularities of the order of $(1/r)$. The usual approach in evaluating these integrals is to extract the singularity contribution analytically and evaluate the Cauchy's principal value numerically. In the present paper the area integrals which assume a linear plastic strain distribution are evaluated analytically over triangular cells. The form of analytical expressions is such that the singularity contribution comes out automatically without the usual need of neglecting the cell (area) containing the singularity. It should be pointed out that the region over which the plastic strain is assumed linear, need not be a triangle. This is especially useful when the general form of the elasto-plastic boundary is known *a priori*, e.g. axisymmetric problems. Good accuracies have been obtained for number of problems. Two examples are included, namely the elasto-plastic deformation of a circular disc with a hole and a square. The circular disc is especially illustrative of the power of the method as the problem is solved in Cartesian coordinates.

1. INTRODUCTION

Several authors[1–6] have extended the boundary integral method to elasto-plastic problems. Most of the formulations, including the present one, consider the plastic strain distribution as analogous to a body force field[8]. In two dimensional elastic problems with no body force fields, the stresses can be written in terms of a line integral over the boundary of the region. This line integral contains unknown functions which are determined finally from the boundary conditions. In the presence of a body force field (unknown plastic-strain distribution in this case) an additional area integral is introduced. It is this area integral that causes the major difficulties in the solution procedure. Since the plastic strains are unknown at each load increment the area of integration (the plastic region) is unknown. Even for assumed known plastic strains, evaluation of the area integral is very difficult. These difficulties are further exacerbated by the fact that the boundary integral equations must be solved for each load increment. Several of these difficulties are addressed in the present paper. These include; an improved evaluation of the boundary integral itself, an improved description of the plastic strain distribution, a numerical evaluation of the singularity contributions in the area integrals, and an improved algorithm for determining the elastic-plastic boundary. The numerical results indicate that the boundary integral method is a viable alternative for elasto-plastic problems.

2. THEORETICAL DEVELOPMENT AND NUMERICAL EVALUATION

The elasto-plastic boundary value problem of interest is shown in Fig. 1. R_P is the plastic zone with elasto-plastic boundary B_P. $R-R_P$ is an elastic region with external boundary B. Note that B, B_P can intersect. Q is an arbitrary field point lying either in R_P or $R-R_P$ where stresses are to be evaluated. P is a point on B where the boundary conditions are to be satisfied. In the present paper only traction boundary conditions are considered.

It has been shown[9,7] for plane strain that the stresses can be expressed;

$$\sigma_{ij}(Q) = \oint H_{ij;k}(Q, P_B) f_k(P_B)\,\mathrm{d}s + \int\int_{R_P} H_{ij;k}(Q, P') F_k(P')\,\mathrm{d}x'\,\mathrm{d}y' - 2Ge^p_{ij}(Q) \quad i,j,k = x,y \tag{1}$$

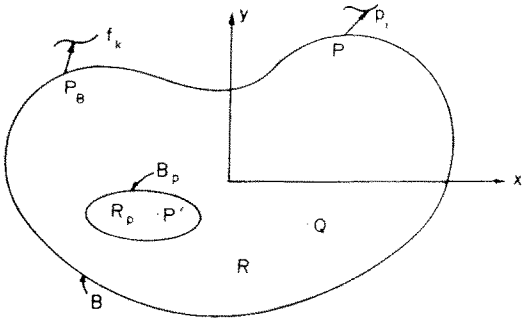

Fig. 1. Elasto–plastic boundary value problem.

$H_{ij;k}(Q,P')$ is an influence function and represents the ijth stress component at a point Q due to a unit concentrated load at P' in the kth direction. The components of $H_{ij;k}$ are given in detail in Ref. [10]. f_k represents a fictitious traction distributed on B and is one of the unknowns in the problem. e_{ij}^p is the incompressible plastic strain distribution in R_P, while F_k (P') is given by;

$$F_k = -2G\, e^p_{kj;j} \tag{2}$$

where the comma implies differention with respect to x, y and G is the shear modulus. Note that F_k has the appearance of a body force field. The plastic strain distribution represents the second set of unknowns in the probelm. For plane stress, the expression for the stresses is the following:

$$\sigma_{ij}(Q) = \oint_B H_{ij;k}(Q,P_B) f_k(P_B)\,\mathrm{d}s + \int\int_{R_p} H_{ij;k}(Q,P')F_k(P')\,\mathrm{d}x'\,\mathrm{d}y' - 2Ge_{ij}^p(Q) - \delta_{ij}2G\frac{\nu'}{1-\nu'}\,e_{kk}^p \quad i,j,k = x,y. \tag{3}$$

Note that in the expression for $H_{ij;k}(Q, P')$ Poisson'r ratio ν should be replaced by $\nu'/(1+\nu')$ where ν' is the value for the plane stress formulation. Also, F_k for plane stress is;

$$F_k = -2G\, e^p_{kj,j} - 2G\frac{\nu'}{1-\nu'}\, e^p_{jj,k}. \tag{4}$$

Since the stresses given by eqns (1) and (3) represent the superposition of fundamental solutions all equations of linear elasticity are satisfied. Note that plasticity can be assumed to be a linear theory within each small load increment. In order to solve the boundary value problem of interest, eqns (1) or (3) must satisfy the boundary conditions on B and the plastic flow rule in R_P (Prandtl–Ruess). The boundary conditions are;

$$\sigma_{ij}(P)\, n_j(P) = p_i(P)\, P \text{ on } B \tag{5}$$

where $n_j(P)$ are the direction cosines of the unit normal to the boundary at P. $p_i(P)$ are the applied traction components at P.

In the usual solution procedure either eqn (1) or (3) is substituted into eqn (5) generating a boundary integral equation. A plastic strain distribution is assumed based on the solution for the previous load step. This entire equation is then discretized producing a set of linear algebraic equation in the unknown f_k. Solving for f_k, stresses can then be found from a discretized version of eqn (1) or (3). These stresses can then be substituted into the plastic flow rule generating a new plastic strain distribution.

The integral equations are solved again and the cycle repeated until convergence of the plastic strain distribution is attained.

A different approach is taken inthe present paper. Equation (1)† is first discretized for Q in R and then substituted into the boundary condition by letting $Q \to P$. This involves the following important ideas which represent the major contribution of the paper.

(1) More detailed boundary subdivisions for both B and B_p.

(2) A combination of piecewise linear and Fourier representations for f_k.

(3) A piecewise linear representation of the plastic strain distribution.

(4) Numerical rather than the usual analytical evaluation of singularity contributions arising both on B and in R_P.

We now proceed with the numerical evaluation of eqn (1). For convenience the following quantities are defined.

$$\sigma_{ij}^{e}(Q) = \oint_B H_{ij;k}(Q, P_B) f_k(P_B)\, \mathrm{d}s \tag{6a}$$

$$\sigma_{ij}^{p}(Q) = \int\int_{R_p} H_{ij;k}(Q, P') F_k(P)\, \mathrm{d}x'\, \mathrm{d}y' - 2Ge_{ij}^{p}(Q) \tag{6b}$$

$$\sigma_{ij}(Q) = \sigma_{ij}^{e}(Q) + \sigma_{ij}^{p}(Q). \tag{6c}$$

The evaluation of the line integral (eqn 6a) has been discussed in detail in Ref. [10] and is discussed here briefly for completeness. The function f_k is assumed piecewise continuous over M segments of the boundary (see Fig. 2). Each of these m segments is then further subdivided into N_m straight line segments. f_k is then expanded about the mid point of these straight line segments using a Taylor series. Retaining the first two terms the integrations can be performed analytically, yielding;

$$\sigma_{ij}(Q) = \sum_{m=1}^{M} \sum_{n=1}^{N_m} \left[M_{ij;k}^{(1)}(Q, S_n) f_k(\bar{s}_n) + \{M_{ij;k}^{(2)}(Q, S_n) - \bar{s}_n M_{ij;k}^{(1)}(Q, S_n)\} \frac{\mathrm{d}f_k}{\mathrm{d}s}(\bar{s}_n) \right] \tag{7}$$

where $M_{ij;k}^{(1)}$ and $M_{ij;k}^{(2)}$ are the first and second integrals of the influence function $H_{ij;k}$ and are given in detail in Ref. [10]. S_n is the value of s at the nth node. $\bar{s}_n$ is defined by $\bar{s}_n = (S_{n+1} + S_n)/(2)$.

A form for f_k is now assumed.

$$\text{Let } f_k = f_{k1} + f_{k2} \tag{8a}$$

where

$$f_k = \frac{d_k^{(m+1)} - d_k^{(m)}}{S_{m+1} - S_m}(s - S_m) + d_k^{(m)}, \quad S_m \leq s \leq S_{m+1} \tag{8b}$$

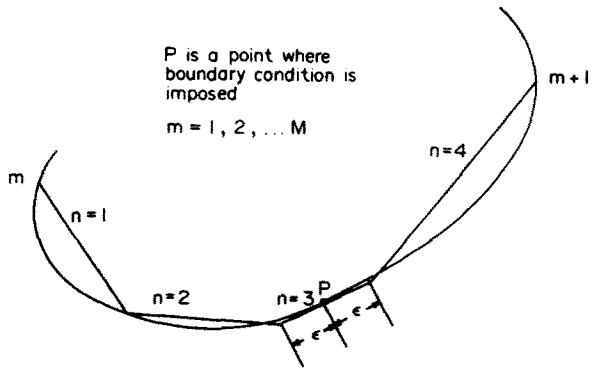

Fig. 2. Example of boundary subdivision ($N_m = 4$).

†Details for the plane strain case only are presented. The analogous plane stress equations will simply be stated.

$$f_{k2} = a_{k0} + \sum_{q=1}^{Q_1} a_{kq} \cos \frac{2\pi qs}{S} + \sum_{q=1}^{Q_2} b_{kq} \sin \frac{2\pi qs}{S} \tag{8c}$$

where S_m is the value of s at the mth node, and S is the length of the discretized boundary.

The piecewise linear representation (8b) is used only in those boundary regions where large gradients in f_k are anticipated, for example, near corners and where the applied load has large gradients. The results in Refs. [9, 10] have shown that a substantial saving is obtained in computer time by use of combination representations over the conventional piecewise linear representation. Note that the further subdivision of the mth segment into N_m parts not only permits the Taylor series approximation but also permits a better representation of the curvature at no increase in the number of unknowns. It should be noted that a_{k0} is retained only for $f_k = f_{k2}$, otherwise a poorly conditioned matrix results, see Ref. [9].

Unlike the line integral, the region of integration for the area integral is not known. However, once the plastic strain distribution is known, the elastic plastic boundary can be found from non-zero values of the plastic strains. This idea, in fact, is used in the previously described iteration cycle, i.e. a plastic strain distribution is assumed which implies the region R_P. To evaluate the area integrals, eqn (6b), two assumptions are made.

The first assumption is that the plastic strains are piecewise linear over each of the N regions R_n of the plastic zone, see Fig. 3.

$$e_{kl}^p = A_{kl}^{(n)} + B_{kl}^{(n)} x + C_{kl}^{(n)} y, \quad x, y \text{ in } R_n \tag{10}$$

$A_{kl}^{(n)} B_{kl}^{(n)} C_{kl}^{(n)}$ are easily solved[9] in terms of the nodal values of the plastic strains. Although the nodal values can be any three non-collinear points, the corners $n1$, $n2$, $n3$ are the usual selections, see Figs. 3 and 4. Substituting eqn (10) into (2);

$$F_x^{(n)} = -2G(B_{xx}^{(n)} + C_{xy}^{(n)}) \tag{11a}$$

$$F_y^{(n)} = -2G(B_{xy}^{(n)} + C_{yy}^{(n)}). \tag{11b}$$

As $B_{kl}^{(n)}$ and $C_{kl}^{(n)}$ are constant over each R_n, $F_k^{(n)}$ is constant over each R_n. Thus, from eqns (11) and (6b)

$$\sigma_{ij}^P(Q) = \sum_{n=1}^{N} F_k^{(n)} \int\int_{R_n} H_{ij;k}(Q,P')\,dx'\,dy' - 2G\,e_{ij}^P(Q) \quad i,j,k = x,y. \tag{12}$$

The second assumption is on the shape of the region R_n. Normally these regions are chosen as triangles except for those cases in which the general form of the elasto-plastic boundary is known, e.g. axisymmetric problems or when the elasto-plastic boundary intersects a curved real boundary, e.g. R_n of Fig. 3. In such cases R_n is further subdivided into a set of M_n triangles (see Fig. 4). This further subdivision permits a better representation of the curvature of elasto-plastic boundary at no increase in the number of unknown plastic strains. That is, more points are used to define the geometry than the plastic strain distribution. It is now possible to perform the integration analytically over each triangle as given in the Appendix.

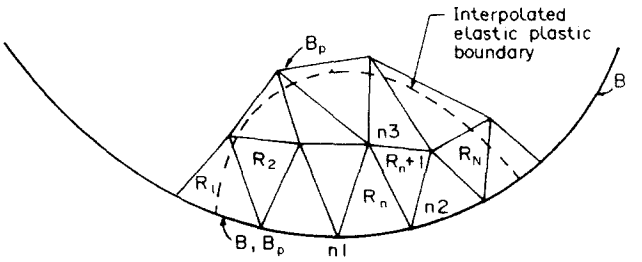

Fig. 3.

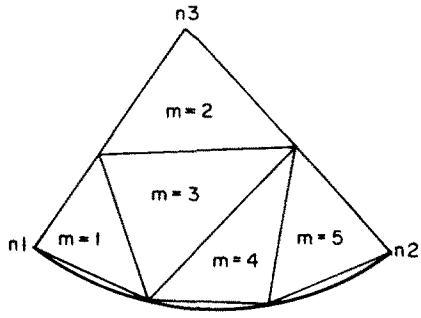

Fig. 4. Further subdivision of $R_n(M_n = 5)$.

The final result is;

$$\sigma_{ij}^{P}(Q) = \sum_{n=1}^{N} F_k^{(n)} \sum_{m=1}^{M_n} J_{ij;k}(Q, R_m) - 2G e_{ij}^{P}(Q) \tag{13}$$

where

$$J_{ij;k}(Q, R_m) = \int_{R_m} \int H_{ij;k}(Q, P')\, dx'\, dy'. \tag{14}$$

In eqn (13) all quantities are known except $F_k^{(n)}$. $F_k^{(n)}$ is related to the nodal values of plastic strain. These nodal values of plastic strain are determined iteratively as described earlier.

In the previous Refs. [1–5] the area integrals have been evaluated by first analytically extracting the singularities present in the field. The plastic strain field is then assumed constant over triangular subintervals. Difficulties are experienced if this approach is extended to the linear plastic strain approximation. There the stress (and strains) must be evaluated at the nodal points of the triangular elements causing difficulties in evaluation of the Cauchy principal values of the integrals. This difficulty is addressed in [11, 12] by a numerical integration scheme. The errors introduced in this scheme due to the approximation of the integrands as well as the difficulties mentioned above are overcome in the present paper by evaluating the integrals analytically for a piecewise linear plastic strain distribution. By taking proper care in the framing the components of $J_{ij;k}$ it is possible to obtain the singularity contribution numerically, see the Appendix. In the author's opinion the present approach also simplifies the computer code.

To determine the plastic zone (and the elasto-plastic boundary) an iteration on the plastic strains is necessary. For this to be efficient, a good first guess is important. In the present work the elastic solution at the given load is used to determine the contour defined by the equivalent stress equal to the yield stress. In general, this underestimates the plastic zone. The zone grows with successive iterations to its final correct size. Precise position of the elastic-plastic boundary is determined by interpolating on the equivalent stress. This approach, initial underestimation, is quite efficient since unnecessary stress computations need not be done.

To complete the formulation the plane stress equivalents of eqns (11) and (13) are given below.

$$F_x^{(n)} = -2G(B_{xx}^{(n)} + C_{xy}^{(n)}) - 2G\frac{\nu'}{1-\nu'}(B_{xx}^{(n)} + B_{yy}^{(n)}) \tag{15a}$$

$$F_y^{(n)} = -2G(B_{xy}^{(n)} + C_{yy}^{(n)}) - 2G\frac{\nu'}{1-\nu'}(C_{xx}^{(n)} + C_{yy}^{(n)}) \tag{15b}$$

and

$$\sigma_{ij}^{(p)}(Q) = \sum_{n=1}^{N} F_k^{(n)} \sum_{m=1}^{M_n} J_{ij;k}(Q, R_m) - 2G e_{ij}^{P}(Q) - \delta_{ij} 2G\frac{\nu'}{1-\nu'} e_{kk}^{P}(Q). \tag{16}$$

3. NUMERICAL EXAMPLES

Two examples are presented to illustrate the above technique. The first is a thin circular disc with a central hole and a uniform tension at the outer radius. This problem is useful for comparative purposes since a closed form solution for the stresses exists[13,14]. It should be noted that the analysis developed in Section 2 does not utilize the symmetry of the problem, i.e. the problem is solved in cartesian coordinate. The second example is that of a thin square section under linearly varying uniaxial tension. This problem is useful for showing the effects of discontinuous loading and corners and also has an exact solution.

Both problems will be solved assuming the dimensionless equivalent stress, equivalent plastic strain relationship;

$$e_p = \sigma_e - 1$$

e_p is non-dimensionalized with respect to the ratio of yield stress to elastic modulus while σ_e is non-dimensionalized with respect to yield stress. This implies a linear strain hardening material with a hardening slope equal to 1/2 the elastic slope. There is no loss of generality for either the assumption of linear strain hardening or the particular choice of slope.

(a) *Example* 1

A quarter section geometry of example 1 is shown in Fig. 5.

The applied traction is;

$$p_x = \begin{cases} 0 & \text{for } r = 1 \\ \alpha_l \cos\theta & \text{for } r = 10 \end{cases} \tag{17a}$$

$$p_y = \begin{cases} 0 & \text{for } r = 1 \\ \alpha_l \sin\theta & \text{for } r = 10 \end{cases} \tag{17b}$$

where α_l is the load parameter nondimensionalized with respect to the yield stress and θ is the angle measured from the x-axis in a counterclockwise direction. The principal stresses are[13,14]

$$\alpha_{rr} = \frac{\alpha_l + A_p}{0.99}\left(1 - \frac{1}{r^2}\right) - \frac{1}{2}\int_1^r g(r)\,dr + \frac{1}{2r^2}\int_1^r r^2 g(r)\,dr \tag{18a}$$

$$\sigma_{\theta\theta} = \frac{\alpha_l + A_p}{0.99}\left(1 + \frac{1}{r^2}\right) - \frac{1}{2}\int_1^r g(r)\,dr - \frac{1}{2r^2}\int_1^r r^2 g(r)\,dr \tag{18b}$$

$$\sigma_{r\theta} = 0$$

where

$$A_p = \frac{1}{2}\int_1^{10} (1 - 0.01r^2) g(r)\,dr \tag{18c}$$

and

$$g(r) = \frac{d}{dr}(e_{\theta\theta}{}^p) + \frac{e_{\theta\theta}{}^p - e_{rr}{}^p}{r} \tag{18d}$$

σ_{rr}, $\sigma_{\theta\theta}$ and $\sigma_{r\theta}$ are the radial, tangential and shear stresses respectively, and $e_{rr}{}^p$ and $e_{\theta\theta}{}^p$ are the radial and tangential plastic strains. To evaluate the integrals in eqn (18), the plastic strains are assumed to vary linearly in small intervals of r. The size of intervals are 0.01 for $1 \leq r \leq 1.5$, 0.1 for $1.5 \leq r \leq 6.5$ and 0.5 for $6.5 \leq r \leq 10$. The problem is solved iteratively as described in Ref. [14] and the solution is then used for comparison with the strsses obtained using the method of Section 2.

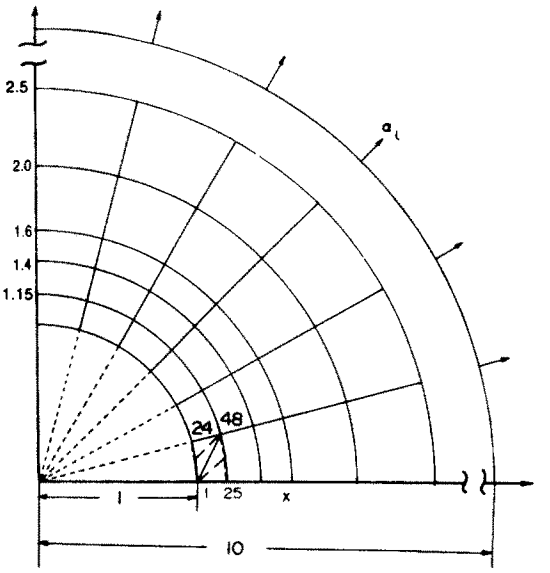

Fig. 5. Example 1; circular disc with central hole.

To solve the problem using the boundary integral method, the unknown function f_k in the line integral is approximated by only a Fourier series, eqn (8c) ($Q_1 = 3$, $Q_2 = 4$), on each boundary. Each boundary is divided into 8 intervals subtending 45°, $M = 16$. Each interval is further subdivided into 12 sub-intervals $N_m = 12$, for all m. The total number of unknowns is 32. The problem is solved for values of the load parameter, (α_l) of 0.495 (initial yield at the inner boundary), 0.6, 0.7, 0.8 and 0.9. Estimates of the zone size for purposes of initiating the iteration cycle at a given load are circle of radius $r = 1$, 1.15, 1.4, 1.6, 2.0 and 2.5. These correspond to the load parameters given above and are based on the elastic solution. This is shown in Fig. 5. On each circle 24 points (nodes) are chosen at which plastic strains are to be determined. Two successive nodes (for example 24 and 1) subtend an angle of 15°. The region bounded by two successive circles and the 15° segment is divided into two regions as shown in Fig. 5 (e.g. region bounded by nodes 24, 1, 48 and 1, 25, 48) and over each of these regions the plastic strains are assumed to vary linearly. Each of these regions is further subdivided into two triangles, ($M_n = 2$). This further subdivision is used for better description of the plastic zone geometry.

Once the convergence of plastic strains is obtained, the stresses are then evaluated along $\theta = 0°$ and $\theta = 22.5°$ for various values of r. Note that evaluating the singularity contribution numerically permits stress evaluations at any point in the region (not just at the node points).

Principal stresses $\sigma_{\theta\theta}$, σ_{rr} are computed from the Cartesian stresses and compared with the known solution. Errors in $\sigma_{\theta\theta}$ for $\theta = 0°$, 22.5°, $1.05 \leq r \leq 9.95$, are less than 0.64% everywhere for load parameters $\alpha_l \leq 0.9$. Error in σ_{rr} are greater particularly near the inner boundary because σ_{rr} must go to zero there. For $\theta = 0$, 22.5, $1.50 < r < 9.95$ errors are approx. 1.0% or less. Near the inner boundary errors in σ_{rr} are greater for $\theta = 22.5°$ since both the boundary condition and plastic strain convergence are satisfied at $r = 1$ and $\theta = 0$, 15°, 30°. In Table 1 the stress concentration factor at $r = 1$ and $\theta = 0°$ is given. The stress concentration factor is

Table 1. Stress concentration factor in example 1

Load Parameter	α_ℓ=0.495	α_ℓ=0.6	α_ℓ=0.7	α_ℓ=0.8	α_ℓ=0.9
Theoretical	2.0202	1.8528	1.7550	1.6948	1.6604
Calculated	2.0251	1.8600	1.7661	1.7064	1.6746
Percentage Error	0.2400	0.3900	0.6300	0.6900	0.8500

defined as the ratio of the tangential stress $\sigma_{\theta\theta}$ on the inner boundary to the load imposed α_l on the outer boundary.

The results show that the variation in elastic-plastic boundary with θ is negligable. It was found that the equivalent stress was not equal to one (yield stress) at any of the mesh circles shown in Fig. 5. The actual location of the elastic plastic boundary for each load was determined by linear interpolation. Following this the plastic radii were found to be; $r_p = 1.000$ $(\alpha_l = 0.495)$, $r_p = 1.157$ $(\alpha_l = 0.6)$, $r_p = 1.341$ $(\alpha_l = 0.7)$, $r_p = 1.620$, $(\alpha_b = 0.8)$, $r_p = 2.124$, $(\alpha_l = 0.9)$.

Table 2 is a summary of computer time and number of iterations. All calculations were done on an Amdhal 470V/8 computer (University of Michigan). Convergence of the plastic strains is defined when all strains for two successive cycles, are within 0.1%.

(b) *Example* 2

The geometry, loading, and interval mesh subdivision for example 2 is shown in Fig. 6.

The applied traction is;

$$p_x = \begin{cases} 0.5\alpha_l\left(1+\frac{y}{5}\right) & x = 5 \qquad -5 \le y \le 5 \\ -0.5\alpha_l\left(1+\frac{y}{5}\right) & x = -5 \qquad -5 \le y \le 5 \\ 0 & -5 \le x \le 5 \qquad y = \pm 5 \end{cases} \tag{19a}$$

$$p_y = 0 \qquad x = \pm 5 \qquad y = \pm 5 \tag{19b}$$

Table 2. Computer time summary and number of iterations in example 1

Matrix Generation Time (in secs)	52.187				
Solution Procedure Time (in secs)	α_ℓ=0.495	α_ℓ=0.6	α_ℓ=0.7	α_ℓ=0.8	α_ℓ=0.9
	4.575	17.850	14.227	31.700	34.355
Number of Iterations	1	6	5	6	6

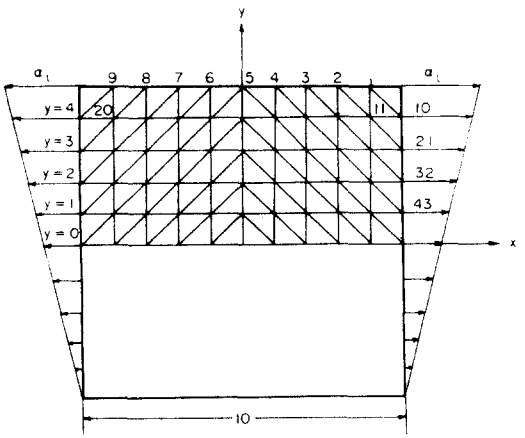

Fig. 6. Example 2; Thin square with linear uniaxial tension.

where α_l is the load parameter again non-dimensionalized with respect to the yield stress. The exact solution is easily found and is given by;

$$\sigma_{xx} = 0.5\alpha_l(1 + (y/5)) \qquad \sigma_{yy} = \sigma_{xy} = 0 \tag{20}$$

and

$$e_{xx}^{\ p} = \sigma_{xx} - 1 \tag{21}$$

$$e_{yy}^{\ p} = -\frac{e_{xx}^{\ p}}{2}; \quad \sigma_{xx} \geq 1$$

$$e_{xy}^{\ p} = 0.$$

The unknown function f_k in the boundary integral is approximated by a combination representation, e.g. (8). Four sine ($Q_1 = 4$), four cosine ($Q_2 = 4$) are used in Fourier series and 80 non-zero values of $d_k^{(m)}$ ($M = 40$) are used in the linear representation. a_{ok} in (8c) is taken as zero as discussed previously. Thus, the total number of unknowns is 96.

Table 3 shows the boundary discretization and location of points where the boundary conditions are to be satisfied along $x = 5$. The other boundaries are identical. Note that at each corner two non-zero values of $d_k^{(m)}$ are permitted.

The problem is solved for load parameter values of $\alpha_1 = 1.00$ (initial yield at the upper edge), (1/0.9), (1/0.8), (1/0.7), (1/0.6). Again, estimates of the zone size for initiating the iteration cycle are based on the elastic solution for the above load parameters. These are horizontal lines at $y = 5, 4, 3, 2, 1, 0$. Based on this the internal discretization is shown in Fig. 6. Plastic strains are assumed to vary linearly over each of the triangles shown in Fig. 6 except for the corners. There, plastic strains vary linearly over the corner squares since the present scheme cannot compute stresses right at the corner.

Stresses are computed along $y = x$ and are compared with the exact solution in Table 4. Negative percentage errors imply the computed solution is less than the exact. Note that the stresses have an error increase near the center. This is partly due to the boundary condition not being satisfied at the midpoint of each side. Also sizeable errors occur near the corners.

In Fig. 7 a comparison of the computed and exact elastic plastic boundary is given for the various load parameters. The computed boundary position is again found by linear interpolation of the equivalent stress between the mesh lines shown in Fig. 6. In Table 5 a computer time summary and required number of interation cycles is given. The convergence criterion is defined as in example 1.

Table 3. Mesh geometry in example 2

m	y-coordinate of points where $d_k^{(m)} \neq 0$	y-coordinate of boundary condition point
1	-5.000	-4.9
2	-4.800	-4.7
3	-4.050	-4.0
4	-3.050	-3.0
5	-2.050	-2.0
6	2.050	-1.0
7	3.050	1.0
8	4.050	2.0
9	4.800	3.0
10	5.000	4.0
11		4.7
12		4.9

Table 4. Percentage error in σ_{xx} in example 2

x=y	$\alpha_\ell=1$	$\alpha_\ell=\frac{1}{0.9}$	$\alpha_\ell=\frac{1}{0.8}$	$\alpha_\ell=\frac{1}{0.7}$	$\alpha_\ell=\frac{1}{0.6}$
0.0	0.20	0.24	1.04	3.03	8.07
0.5	0.13	0.31	1.53	4.20	7.18
1.0	0.08	0.37	2.01	5.36	5.18
1.5	0.02	0.43	2.50	4.50	3.62
2.0	-0.03	0.48	2.99	4.31	1.25
2.5	-0.08	0.54	2.40	1.53	- 0.55
3.0	-0.14	0.63	2.40	-0.36	- 1.53
3.5	-0.24	0.51	0.24	-1.23	- 1.76
4.0	-0.50	0.60	-1.04	-1.53	- 1.81
4.5	-1.85	-2.25	-2.27	-2.71	- 3.49
4.6	-2.78	-3.25	-3.23	-3.74	- 4.61
4.7	-4.40	-4.92	-5.06	-5.65	- 6.55
4.8	-7.22	-7.81	-8.37	-9.12	-10.02

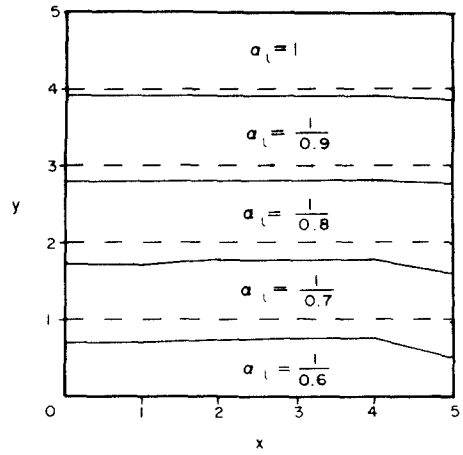

Fig. 7. Elastic plastic boundaries in example 2, ----- exact, ——— boundary integral method.

The examples above demonstrate that the boundary integral method when properly formulated is a viable alternative for the solution of elasti-plastic problems. The numerical improvements developed in this paper namely; numerical extraction of the singularity contribution both internally and on the boundary, subinterval surface and boundary discretization for better geometry description, linear plastic strain representation, combination representation (Fourier plus linear) of the fictitious traction distribution, and the improved estimate of the

Table 5. Computer time summary and number of iterations in example 2

Matrix Generation Time (in secs)	28.059				
Solution Procedure Time (in secs)	$\alpha_\ell=1$	$\alpha_\ell=\frac{1}{0.9}$	$\alpha_\ell=\frac{1}{0.8}$	$\alpha_\ell=\frac{1}{0.7}$	$\alpha_\ell=\frac{1}{0.6}$
	2.799	12.560	27.311	33.413	35.522
Number of Iterations	1	12	22	25	21

plastic zone all demonstrate the importance of attention to numerical detail in developing an efficient, accurate code.

The above ideas can be extended to higher order shape functions for plastic strains. To do this; analytical expressions for the integrals of the influence function H_{ijk} with higher order terms must be obtained. The reasons which lead the authors to believe that these analytical expressions can be found are as follows.

The function $I_{ij;k}$ (see Appendix, e.g. A1) consists of a linear combination of three types of functions, namely a logrithmic function, tan inverse function and functions which when integrated the second time produce the first two functions. Further integration of logrithmic and tan inverse function produce more logrithimic and tan inverse functions. Hence by successive use of Green's theorem it is possible to obtain a line integral over the boundary of the triangle. By transforming to the local coordinate system mentioned in the Appendix, analytical expressions for the integrals of the influence function can be obtained.

It is obvious from the above discussion that a lot more work needs to be done when a scheme is based on analytical integration rather than on numerical integration. In the opinion of the authors, the saving in computer time and the higher accuracies which generally results from analytical integration justifies this extra effort.

REFERENCES

1. J. L. Swedlow and T. A. Cruse, *Int. J. Solids Structures* 7, 1673–1683 (1971).
2. A. Mendelson, Boundary integral method in elasticity and plasticity. NASA TN D-7418, 1973.
3. V. Kumar and S. Mukherjee, *Int. J. Mech. Sci.* 19, 713–724 (1977).
4. H. D. Bui, *Int. J. Solids Structures* 14, 935–939 (1978).
5. P. C. Riccardella, An implementation of boundary integral technique for planar problems in elasticity and elasto-plasticity. Rep. SM-7310, Department of Mechanical Eng., Carnegie Mellon University, Pittsburg, PA, 1973.
6. P. K. Banerjee and D. N. Cathie, *Int. J. Mech. Sic.* 22, 233–245 (1980).
7. R. Benjumea and D. L. Sikarskie, *J. Appl. Mech.* 4, 801–808 (1972).
8. T. H. Lin, *Theory of Inelastic Structures.* Wiley, New York (1968).
9. M. Vable, An algorithm for evaluating the boundary integral equations in planar elasto-plastic bodies. Ph.D. Dissertation, University of Michigan, Ann Arbor, MI, 1981.
10. M. Vable and D. L. Sikarskie, *Comput. Structures* 14, 29–35 (1981).
11. J. C. F. Telles and C. A. Brebbia, *Appl. Math. Modelling* 3, 466–470 (1979).
12. M. Morjaria and S. Mukerjee, *Int. J. Solids Structures* 17, 127–143 (1980).
13. I. S. Tuba, *J. Appl. Mech.* 710–711 (1965).
14. A. Mendelson, *Plasticity: Theory and Application.* Macmillan, New York (1969).

APPENDIX

Definition of $J_{ij;k}$ and the numerical evaluation of the singularity contribution:

The function $J_{ij;k}$ represents the integrals of the influence function $H_{ij;k}$ over a triangle. The important steps in obtaining the components of $J_{ij;k}$ are outlined briefly. First the function $I_{ij;k}$ are determined such that

$$H_{ij;k} = \frac{\partial I_{ij;k}}{\partial x'}. \tag{A1}$$

By use of Green's theorem, the surface integral is then written in terms of a line integral over the boundary of the triangle. This line integral can be evaluated by transforming the global coordinate system to a local coordinate system of tangential and normal components over each side of the triangle. Let BC (see Fig. 8) represent one of the sides of a triangle bounded by nodes p and q.

By geometry it can be shown that

$$h_{qp} = -(r_{xq} \sin \theta_{qp} - r_{yq} \cos \theta_{qp}) \tag{A2a}$$

$$S_{qp} = -(r_{xq} \cos \theta_{qp} + r_{yq} \sin \theta_{qp}) \tag{A2b}$$

where r_{xq}, r_{yq}, are the components of r_q. r_q is positive when directed toward Q. The components of $J_{ij;k}$ can be shown to be, see Ref. [9].

$$J_{xx;x} = -\frac{a_1 - a_2}{16\pi}\Phi^{(3)} - \frac{3a_1 + a_2}{16\pi}\Phi^{(1)} \tag{A3a}$$

$$J_{xx;y} = \frac{a_1 - a_2}{16\pi}\Phi^{(4)} + \frac{5a_2 - a_1}{16\pi}\Phi^{(2)} \tag{A3b}$$

$$J_{yy;x} = \frac{a_1 + a_2}{16\pi}\Phi^{(3)} + \frac{5a_2 - a_1}{16\pi}\Phi^{(1)} \tag{A3c}$$

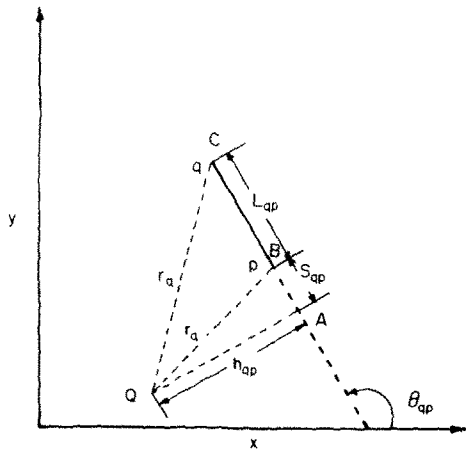

Fig. 8. Geometry needed for evaluation of $J_{ij;k}$.

$$J_{yy;y} = -\frac{a_1 - a_2}{16\pi}\Phi^{(4)} - \frac{3a_1 + a_2}{16\pi}\Phi^{(2)} \tag{A3d}$$

$$J_{xy;x} = \frac{a_1 - a_2}{16\pi}\Phi^{(4)} - \frac{a_1 + 3a_2}{16\pi}\Phi^{(2)} \tag{A3e}$$

$$J_{xy;y} = \frac{a_1 - 3a_2}{16\pi}\Phi^{(3)} - \frac{a_1 + 3a_2}{16\pi}\Phi^{(1)} \tag{A3f}$$

where

$$J_{xy;y} = \frac{a_1 - a_2}{16\pi}$$

where

$$\Phi^{(l)} = \phi_{21}^{(l)} + \phi_{32}^{(l)} + \phi_{13}^{(l)} \quad l = 1,2,3 \text{ and } 4 \tag{A4}$$

and

$$\phi_{qp}^{(1)} = -h_{qp}\left(\sin\theta_{qp}\beta_{qp} + \cos\theta_{qp}\log\frac{r_q}{r_p}\right) \tag{A5a}$$

$$\phi_{qp}^{(2)} = -h_{qp}\left(\sin\theta_{qp}\log\frac{r_q}{r_p} - \cos\theta_{qp}\beta_{qp}\right) \tag{A5b}$$

$$\phi_{qp}^{(3)} = -h_{qp}\left(\sin 3\theta_{qp}\beta_{qp} + \cos 3\theta_{qp}\log\frac{r_q}{r_p}\right) + \frac{L_{qp}}{2}\sin 3\theta_{qp} \tag{A5c}$$

$$\phi_{qp}^{(4)} = -h_{qp}\left(\sin 3\theta_{qp}\log\frac{r_q}{r_p} - \cos 3\theta_{qp}\beta_{qp}\right) + \frac{L_{qp}}{2}\cos 3\theta_{qp} \tag{A5d}$$

and

$$\beta_{qp} = \tan\frac{-1S_{qp} + L_{qp}}{h_{qp}} - \tan^{-1}\frac{S_{qp}}{h_{qp}}.$$

When the point Q is on one of the corners of the triangle, the radial distance r goes to zero, and the function $H_{ij;k}$ tends to infinity. In the function $J_{ij;k}$ the term that will tend to infinity when the radial distance goes to zero is the logrithmic term. However, this logrithmic term is being multiplied by the perpendicular distance h_{qp} which also becomes zero when the point Q is on the line bounded by nodes q and p. Thus the function $J_{ij;k}$ is always bounded. In the computer programs the terms being multiplied by h_{qp} are not evaluated whenever h_{qp} is zero. When the point Q is inside or outside the triangle, all terms appearing in eqns (A3)–(A5) are defined. Another important piece of information is obtained from the sign of h_{qp}. It can be easily verified that when point Q is either on the boundary of the triangle or in the triangle, all h_{qp} (i.e. h_{21}, h_{32} and h_{13}) are of the same sign. If the point Q is outside the triangle, then one of the h_{qp}'s has a different sign. This information is used to determine when the term $2Ge_{ij}^{p}(Q)$ must be subtracted from the stress expression $\sigma_{ij}^{p}(Q)$ in eqn (13).